The electrical conductivity and thermal electromotive force of lithium hydride and lithium deuteride at 20-50 GPa

1993 J. Phys.: Condens. Matter 5 8659

(http://iopscience.iop.org/0953-8984/5/46/005)

J. Phys.: Condens. Matter 5 (1993) 8659–8664. Printed in the UK

The electrical conductivity and thermal electromotive force of lithium hydride and lithium deuteride at 20–50 GPa

A N Babushkin†, G I Pilipenko‡ and F F Gavrilov‡

† Department of Physics, Ural State University, 620083 Ekaterinburg, Russia

‡ Department of Physics, Ural State Technical University, 620002 Ekaterinburg, Russia

Received 1 December 1992, in final form 21 April 1993

Abstract. It has been shown that insulating LiH and LiD transform gradually to a semiconducting state at about 30 GPa and room temperature. It was also found that these compounds undergo a semiconductor-to-semimetal transition at about 43 GPa. The observed phenomena can probably be explained by a first-order phase B1-to-B2 structure transition.

1. Introduction

Both lithium hydride and lithium deuteride occupy a special place among the binary ion crystals of AB type with the NaCl (B1) crystal structure; this is explained as due to the filling of the anion H^- (D^-) $1s^2$ and cation Li^+ $1s^2$ electron shells [1]. This involves marked differences in the physical properties; among other features the electrical conductivity of these compounds is characteristically different from that of typical binary ion crystals.

The electrical conductivity of LiH at ambient pressures and high temperatures has been studied in detail [2–8]. It has been found that some disagreement between the experimental results of various workers can be explained by the crystal composition and perhaps by the changeability of the hydrogen state as has been shown in [9].

High pressures while causing a crystal volume decrease also result in an increase in the overlapping of the considerably delocalized wavefunctions and total delocalization of the hydrogen anion electrons, i.e. this leads to LiH electron spectrum metallization. Theoretical calculations of this transition pressure have given a value of 2300–5500 GPa [10–12]. Subsequently, it was reported that the LiH undergoes a transition from an insulator state to a semimetal state as a result of the X_1–X_4 energy gap closure which is possible at pressures of the order of 250 GPa [13, 14]. The calculations in [10–19] have been performed assuming that low- and high-pressure phases have the same crystal structures (B1 type). Comparatively low pressures of about 50 GPa of the insulator-to-metal transition have been predicted in [16].

In his theoretical paper, Kulikov [14] suggests the possibility of a LiH transition induced by pressures of 50–100 GPa from a NaCl (B1)-type structure to the CsCl (B2)-type structure (characteristic for many binary ion crystals). A LiH energy-band-structure calculation with the hypothetical B2 structure has shown the possibility of existence of a nearly overlapping indirect gap X–R in the electron spectrum [14]. This means that the pressure-induced phase B1-to-B2 structure transition in LiH (if it really exists) must be accompanied by a considerable increase in conductivity.

The aim of this paper is to study experimentally the electron properties of LiH and LiD under high static pressures at which it should be possible to observe the predicted

0953-8984/93/468659+06$07.50

theoretically changes in the phase and electron structures. For this purpose, measurements of the resistance temperature dependences between 80 and 300 K and between 20 and 50 GPa and the pressure dependence of thermal electromotive force (TEMF) have been made.

2. Experimental procedure

The LiH and LiD compounds possess the rocksalt crystal structure; the lattice parameters are 0.4084 nm and 0.4068 nm, respectively. Single crystals of LiH and LiD were grown from the melt by the Bridgman–Stockbarger method. The total amounts of uncontrolled impurities in the synthesized samples were less than 0.001 wt%. Specimens of about 0.1 mm width were cleaved along the crystal [100] axis.

High pressures have been generated in the diamond anvil cell (DAC) with anvils of the 'rounded cone–plane' type made of synthetic carbonado-type diamonds [15]. These diamonds are good conductors, permitting us to measure the resistance temperature and pressure dependences and the TEMF of the sample placed between the anvils in the DAC using the anvil as the electrical contacts to the sample. The DAC resistivity without the sample is several ohms in magnitude and increases slightly in the temperature range 4.2–400 K. Thus, if we study the kinetic properties of samples whose resistivity is greater than the resistivity of the DAC without a sample, the anvils will not significantly influence the dependences under study.

Control measurements of the TEMF have been made on Cu and Si samples. They are in good agreement with the data obtained by other workers [17].

The estimation of pressure in our DAC is not easy since the pressure obtained depends on the elastic properties of the compressed layer and anvils as well as on the anvil geometry. The procedure for estimation of the pressure reached in a DAC of the 'rounded cone–plane' type has been described in previous work [18]. The pressure values given below have been estimated with the help of the equation

$$P = AF/\pi a^2 \tag{1}$$

where A is an empirical factor equal to 1.51, F is the force applied and a is the radius of spot contact defined by the relation

$$a^4 - 3Fr(1-\mu_2^2)/4E_2 - (0.14Fr/E_1\mu_1^{0.74})\delta = 0. \tag{2}$$

In (2), r is the sphere radius, E is Young's modulus, μ is Poisson's ratio, the subscript 1 corresponds to the layer, the subscript 2 corresponds to the semispace and δ is the elastic layer thickness.

Although equation (2) was originally derived in the axially symmetric problem of elasticity theory, the case of a perfectly rigid-sphere contact with a two-layered base—a thin layer on an infinite elastic semispace [19], it was later shown to be applicable to pressure estimation in a DAC with 'rounded cone–plane'-type anvils [18].

The elastic layer thickness value used in these calculations has been measured with an interference microscope. The radius of the conic anvil curvature has been measured with a micrometer microscope. The different thicknesses of the LiH and LiD samples measured at the position of anvil contact after the pressure treatment are 0.8–1.5 μm.

3. Results and discussion

On measurement of the LiH and LiD resistance pressure dependences it has been found that above 30 GPa for LiH and above 27 GPa for LiD the sample resistance decreases dramatically from the value of 100 MΩ corresponding to the non-conducting state of the samples (this being determined by the shunt influence of the measuring devices) to the value 1–100 kΩ (figure 1).

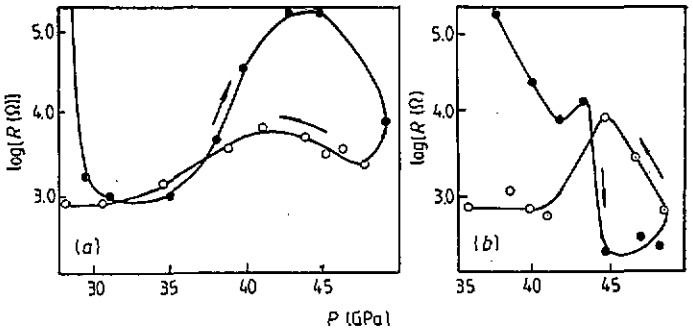

Figure 1. The resistances of (*a*) LiD and (*b*) LiH as functions of pressure.

When the pressure decreases, the reverse transition from a conducting state to an insulating state takes place and the pressures of the direct and reverse transitions do not coincide. According to our estimation, LiH and LiD change to the insulating state below 20 GPa. We should note that after decreasing the pressure to zero and subsequently loading the DAC the resistance pressure dependences of the samples under study can be reproduced with good accuracy, which shows the absence of decomposition induced by pressure. A similar pressure resistance hysteresis has been observed earlier in a study of NaCl [20] and other alkali-metal halides. In our opinion this is connected with the appearance of metastable states characteristic of phase transformations of the first kind. This conclusion also corroborates the observed metastable phase'defreezing' effect which is also analogous to that described in [21].

As has been stated above, according to the theoretical estimation a structural transition from phase B1 to phase B2 is possible in LiH at 50–100 GPa and must be accompanied by a dramatic conductivity increase [14]. The observed transition of LiH and LiD to a state with high conductivity is found at a pressure close to this theoretical estimation and is accompanied by a considerable pressure hysteresis, thus giving us grounds to suppose that there is a B1-to-B2 structural transition above 30 GPa in LiH and LiD.

Figures 2 and 3 show the resistance temperature dependences of the compounds under study. Just after the transition to the high-conductivity state these dependences are described by the usual equation.

$$R = R_0 \exp(E_a/kT) \tag{3}$$

characteristic of non-degenerate semiconductors with the activation energy for conductivity being constant in the whole of the temperature interval 80–300 K (figures 2(*a*) and 3(*a*)). The activation energy under various pressures was obtained by a least-squares fit to equation (3). As shown in figure 4 the activation energy changes non-linearly with increasing

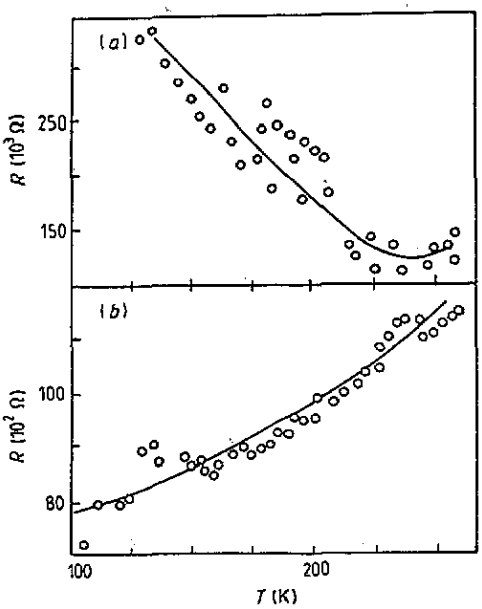

Figure 2. The dependences of resistance on temperature for LiD at (*a*) 39 GPa and (*b*) 45 GPa.

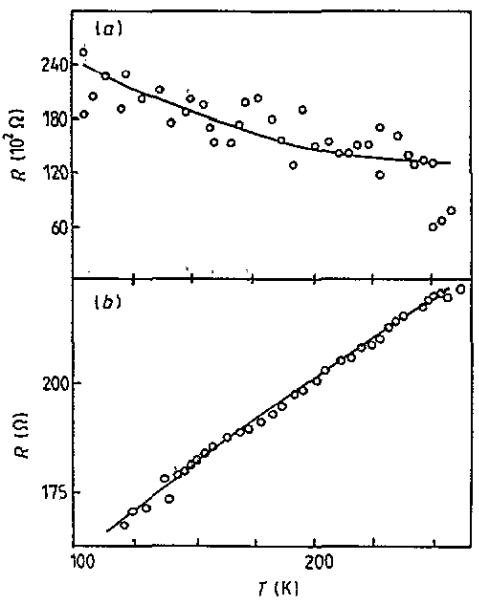

Figure 3. The dependences of resistance on temperature for LiH at (*a*) 43 GPa and (*b*) 47 GPa.

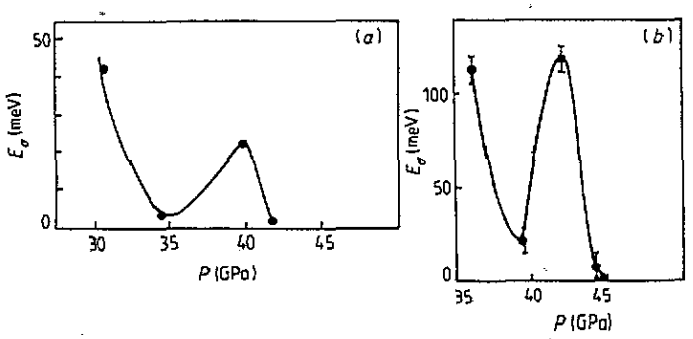

Figure 4. The variation in conductivity activation energy with pressure for (*a*) LiD and (*b*) LiH.

pressure. At pressures above 44 GPa for LiH and above 41 GPa for LiD the resistance temperature dependence changes and it becomes typical for degenerate semiconductors, semimetals or metals. A resistivity estimation from our experimental results (in this state at 300 K) gives 7 Ω m for LiH and 300 Ω m for LiD.

Figure 5 shows the pressure dependences of the differential TEMFs of LiH and LiD. It is well known [22] that in the case of a degenerate semiconductor the TEMF depends on the chemical potential E_F and temperature as given by the relationship

$$S = -(\pi^2 k^2 T/3eE_F)(b + \tfrac{3}{2}) \tag{4}$$

where k is the Boltzmann constant, e is the electron charge and b is a parameter determined by scattering due to acoustic phonons ($b = -0.5$ [22]).

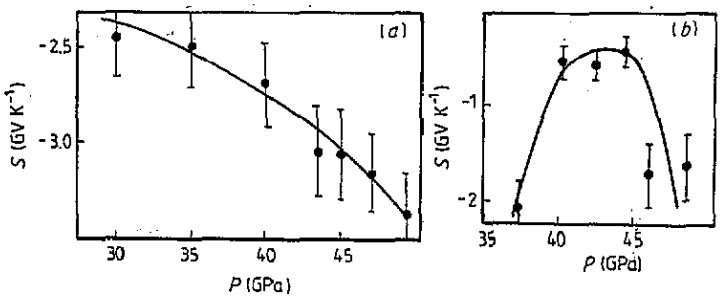

Figure 5. The TEMFs of (*a*) LiD and (*b*) LiH as functions of pressure.

Using (4) it is possible to estimate the value of the chemical potential (Fermi energy) of the phase with a positive temperature coefficient of resistance and, from it, the conductivity electron (or hole) concentration

$$n = (2E_F m)^{3/2}/3\pi^2 h^3 \tag{5}$$

where h is the Planck constant and m is the effective mass (in our estimation, the free-electron mass). In conformity with (4) and (5), estimations give $E_F = 4.4 \pm 0.7$ eV and $n = (4 \pm 1) \times 10^{28}$ m^{-3} for LiH at pressure above 43 GPa, and $E_F = 2.3 \pm 0.2$ eV and $n = (1.6 \pm 0.2) \times 10^{28}$ m^{-3} for LiD above 41 GPa.

If our supposition that, at pressures of the order of 30 GPa, LiH and LiD undergo a structural transition of phase B1 to phase B2 holds true, the energy band diagram given in [14] may be used to interpret the results obtained (figure 6).

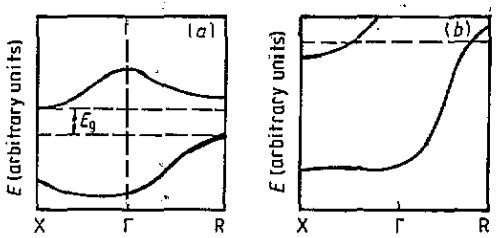

Figure 6. Energy band diagram of LiH(D) with a CsCl structure in (*a*) the semiconducting state and (*b*) the semimetal state.

The dependence of the electrical conductivity on the activation energy at 30–44 GPa for LiH and 27–41 GPa for LiD is probably determined by the thermal excitation of electrons from the top of the valence band at point R to the conduction band at point X. The conductivity activation energies correspond to the indirect gap between these two points (the gap width is connected to the conductivity activation energy by the relationship $E_g = 2E_a$). A decrease in the conductivity activation energy with pressure increase between 35 and 39 GPa for LiH and between 27 and 35 GPa for LiD is connected to the decrease in the energy gap X–R with increasing pressure.

The fact that there is a maximum in the resistivity and conductivity activation energy pressure dependences may be due to two possible mechanisms. First, this maximum may be due to non-parabolicity of the energy bands. While these energy bands are filled with charge carriers, the effective mass of the latter should increase [23]. Second, at small values of E the formation of excitons is possible when $E_g - E_b < 0$, where E_b is the exciton bond energy [24].

Above 44 GPa for LiH and above 41 GPa for LiD the indirect gap X–R is equal to zero and the conductivity is determined by both the electrons at point X and the holes at point R of the Brillouin zone; this means that two-zone semimetals appear. The TEMF and resistivity (and its pressure and temperature dependences) are determined by the summed contribution of the two charge carrier groups.

4. Conclusion

The study of the electrical conductivity of LiH and LiD at 80–300 K and 20–50 GPa and the pressure dependences of the TEMF has shown that at pressures of the order of 30 GPa these compounds transform to a semiconducting state. Above 44 GPa for LiH and above 41 GPa for LiD these compounds undergo a semiconductor-to-semimetal transition. The conductivity at these pressures is probably determined by the types of carrier. The data obtained are in agreement with the theoretical calculations made earlier.

Acknowledgments

The authors would like to thank Professor L Ya Kobelev, Professor E N Yakovlev and Professor S S Batsanov for encouragement and support of this work.

References

[1] Lushnik Ch B, Gavrilov F F, Zavt G S, Plekhanov V G and Cholakh S O 1985 *Electronic Excitations and Defects in Lithium Hydride Crystals* (Moscow: Nauka) p 3 (in Russian)
[2] Pretzel F E, Ruppert G N, Mader C L *et al* 1960 *J. Phys. Chem. Solids* **46** 10
[3] Varotsos P and Mourikis S 1974 *Phys. Rev.* B **10** 5220
[4] Varotsos P 1976 *J. Physique Coll.* **37** C7 327
[5] Ikeya M 1977 *J. Phys. Soc. Japan* **42** 168
[6] Ptashnik V B, Dunaeva T Yu and Baikov Yu M 1982 *Phys. Status Solidi* b **110** K121
[7] Baikov Yu M, Dunaeva T Yu and Ptashnik V B 1981 *Fiz. Tverd. Tela* **23** 2504
[8] Pilipenko G I, Oparin D V and Zhuravlev N A 1987 *Izv Akad. Nauk SSSR, Ser. Neorg. Mater.* **23** 562
[9] Baikov Yu M and Dunaeva T Yu 1982 *Zh. Fiz. Chim.* **56** 1769
[10] Behringer R E 1959 *Phys. Rev.* **113** 787
[11] Trubitsyn V P and Ulinich F R 1963 *Izv. Akad. Nauk SSSR, Ser. Geofiz.* **6** 949
[12] Berggren K-F 1969 *J. Phys. C: Solid State Phys.* **2** 802
[13] Perrot F 1976 *Phys. Status Solidi* b **77** 517
[14] Kulikov N I 1978 *Fiz. Tverd. Tela* **20** 2027
[15] Yakovlev E N, Vinogradov B W, Stepanov G N and Timofeev Yu A 1980 *Rev. Phys. Chem. Japan* **50** 243
[16] Vaisnus J R and Zmuidzinas J S 1978 *Appl. Phys. Lett.* **32** 152
[17] Stshennikov V V 1988 *Rasplavy* **2** 823
[18] Babushkin A N 1992 *High Pressure Res.* **6** 349
[19] Makushkin A P 1984 *Trenie Iznos* **5** 823
[20] Babushkin A N, Kodelev L Ya, Babushkina G V and Yakovlev E N 1991 *Inorg. Mater.* (Engl. Transl.) **27** 301
[21] Verechagin L F, Yakovlev E N, Vinogradov B V, Sakun V P. 1975 *Pribory Tekn. Exp.* **5** 205
[22] Bontch-Bruevitch B L and Kalashnikov S F 1977 *Fizika Poluprovodnikov* (Moscow: Nauka) p 672
[23] Tsidilkovski I M 1972 *Elektrony i Dyrki v Poluprovodnikakh* (Moscow: Nauka) p 449
[24] Madelung O 1985 *Fizika Tverdogo Tela: Lokazovannye Sostoyania* (Moscow: Nauka) p 53 (transl. of Madelung O 1978 *Introduction to Solid State Theory* (Berlin: Springer))